

Study the Combination of Photovoltaic Panels With Different Auxiliary Systems in Grid-Connected Condition

S. Sadeghi¹

Department of Mechanical Engineering,
Graduate University of Advanced Technology,
Kerman, Iran
e-mail: s.sadeghi@kgut.ac.ir

M. Ameri

Department of Mechanical Engineering,
Shahid Bahonar University,
Kerman, Iran
e-mail: ameri_mm@yahoo.com

This study considers the effect of PV panel cost on the use of auxiliary power systems (APSs) in the hybrid power generation system for grid-connected condition. Using the auxiliary power systems along with the PV panels is not essential in grid-connected condition; furthermore, auxiliary power systems produce emission. Therefore, if using the APS is not economic, the use of them is not justifiable. If their use can be justified, a comparison should be made between different auxiliary systems in order to choose the best among. In this work, an evolutionary algorithm (Pareto envelope-based selection algorithm (PESA)) is used for the comparison of different auxiliary systems. In addition, the effect of seasonal and monthly changes of the panel angle is considered. Seasonal or monthly change of the panel angle can improve the PV panel productivity and decrease the annualized cost (ANC) of the power generation system. In addition, this study examines the economical effect of unit electricity power price on the power exchange rate of the hybrid system with grid utility. [DOI: 10.1115/1.4027696]

Keywords: grid-connected, multi-objective optimization, PV panel, hybrid system, auxiliary power system

1 Introduction

The energy from sunlight reaching the earth is a huge potential that can be exploited and used for generating electricity. The ever-increasing energy consumption, the exhaustible nature of fossil fuel, and the worsening global environment have created booming interest in renewable energy source power generation systems. Discontinuity due to the energy produced by solar panels necessitates using the photovoltaic (PV) panels in combination with an auxiliary power system. Because of this, hybrid energy systems have caught worldwide research attention. It is noted that there are many combinations of different alternative energy sources and storage devices to build a hybrid system. A hybrid alternative energy system can either be stand-alone or grid connected.

For a stand-alone application, the system needs to have sufficient storage capacity to handle power variations from the involved alternative energy sources. Bernal-Agust and Duflo-Lopez [1] revised the simulation and optimization techniques and the tools existing that are needed to simulate and design stand-alone hybrid systems for the generation of electricity. Baniasad Askari and Ameri [2] studied a simple optimization method for calculating the optimum configurations of photovoltaic-battery (PV-bat) systems with high reliability and minimum cost. The proposed method had been applied to design a PV-bat system to supply a typical load requirement in a remote region in Kerman, Iran.

Some power generation systems that can be associated with this system are diesel generator (DG), gas generator (GG), micro-gas turbine (MGT), and solid oxide fuel cell (SOFC). Diesel generators give relatively high efficiency. These devices change

the diesel combustion energy to electricity. The combination of diesel generators with solar panels and batteries are often used. Dufo-Lopez and Bernal-Agust [3] optimized a PV-diesel system by hybrid optimization by genetic algorithms (HOGA) program and compared it with a stand-alone PV-only system. The results show the economical advantages of the PV-hybrid system. A recent study used the HOMER software to perform the techno-economic feasibility of hybrid PV/diesel energy system and demonstrated the impact of PV penetration and battery storage on energy production, cost of energy, and number of operational hours of diesel generators for a given hybrid configurations [4]. Baniasad Askari and Ameri [5] used PV-diesel-battery power systems to meet typical load requirements in a remote region in Kerman, Iran. They used a simple optimization method to determine the systems with high reliability and low cost. Morega and Tudorache [6] designed an optimal integrated hybrid system for autonomous electric power production, based on the concurrent operation of a wind turbine and a PV system, backed up by a diesel generator. The optimization of the proposed hybrid system is based on the logistic type numerical models implemented in the HOMER software package.

Owing to the price and availability of natural gas (NG) in Iran, the use of gas generator is suitable. The combination of a gas generator with solar panels has not been considered so far. In this study, this combination will be compared with other combinations.

Microgas turbines have recently been considered especially in combination with other devices. Degobert et al. [7] studied the possibility of using a photovoltaic system combined with a high speed microturbine. They considered the electrical aspect.

Fuel cells are under development. They have relatively high efficiency, low noise (they do not have movement components), and little emission. Silva and coworkers [8] presented an economical assessment and optimization of a hybrid distributed generation system, comprising a PV system, proton exchange membrane

¹Corresponding author.

Contributed by the Solar Energy Division of ASME for publication in the JOURNAL OF SOLAR ENERGY ENGINEERING. Manuscript received March 9, 2014; final manuscript received May 7, 2014; published online May 29, 2014. Assoc. Editor: Santiago Silvestre.

(PEM) fuel cell, and batteries as a potential source of energy for isolated communities in the Amazon region. Eroglu et al. [9] proposed a photovoltaic/wind/PEM fuel cell hybrid power system for stand-alone applications demonstrated with a mobile house. They showed that different renewable sources can be used simultaneously to power off-grid applications.

For a grid-connected mode, the alternative energy sources can supply power both to local loads and to the utility grid. The storage device for these systems can remove, since the grid can be used as a system backup. However, when connected to a utility grid, important operation and performance requirements, such as voltage, frequency, and harmonic regulations, are imposed to the system. Controllers suitable for both grid-connected and stand-alone applications are being developed and implemented in inverters, which could support the operation of hybrid system [10,11].

Türkay and Telli [12] selected a pilot region and introduced cost analysis of using renewable energy sources with a hydrogen system for that region's energy demand, in a technoeconomic perspective. Liu et al. [13] investigated the economic, technical, and environmental performance of the residential PV system running under the Queensland (Australia) climatic conditions and optimized the size and slope of PV array in the system.

Because of the large number of variables usually considered and the mathematical models applied, classical optimization techniques may consume excessive CPU time or even prove unable to take into account all the characteristics associated with the posed problem. During the last three decades, heuristic techniques have been applied. One of the most used heuristic techniques has been the multi-objective evolutionary algorithms (MOEAs). Dufo-Lopez and Bernal-Agust [14] applied the strength of Pareto evolutionary algorithm to the multi-objective design of isolated hybrid systems, minimizing both the total cost and the unmet load. They also studied a triple multi-objective design of the isolated PV-wind-diesel-hydrogen-battery system that minimized, simultaneously, the total cost throughout the useful life of the installation, pollutant emissions (CO₂), and unmet load by a MOEA and a genetic algorithm (GA) [15]. Sadeghi and Ameri [16] presented a multi-objective optimization method for calculating the optimum configurations of photovoltaic-battery systems with high reliability and minimum cost for different tilt angle of panels.

In this study, the effect of applying a power system in combination with PV panels for supplying a sample load in grid-connected condition is considered. Different power systems are compared to select the best system as auxiliary power system. This comparison is made by a multi-objective evolutionary algorithm. Objective functions are annualized cost and CO₂ emission. In addition, the effect of monthly and seasonal changes of panel angle is discussed. From the point of view of power exchange rate, power generation system can connect to grid utility in several ways. In this study, the best situation would be researched.

2 Load Demand

In the present work, load demand is a collection of 500 households in Kerman. The measured annual average electric energy consumption of 500 typical households is considered. The household energy consumption data have been obtained from Kerman Electric Power Distribution Company. The diagram of sample load has been plotted in Fig. 1, which shows mean electrical load for every month.

Different situations are considered for connection between power generation system and electricity grid:

- 0%: Bought electricity power and sold electricity power are equal.
- 10%: Sold electricity power is 90% of bought electricity power.
- 20%: Sold electricity power is 80% of bought electricity power.

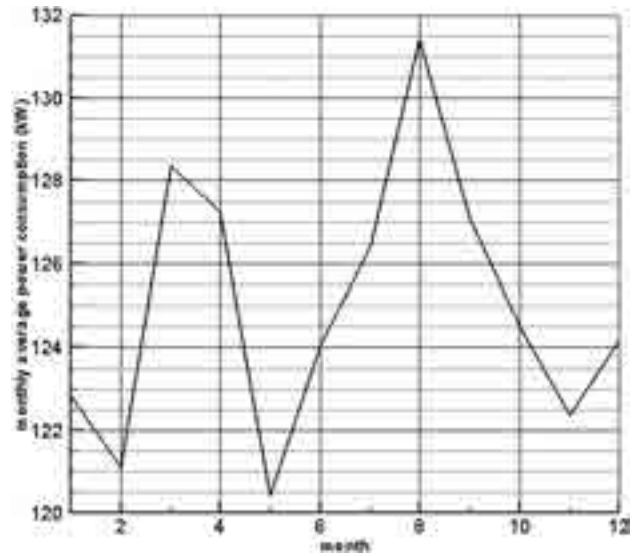


Fig. 1 Monthly average power consumption for 500 households

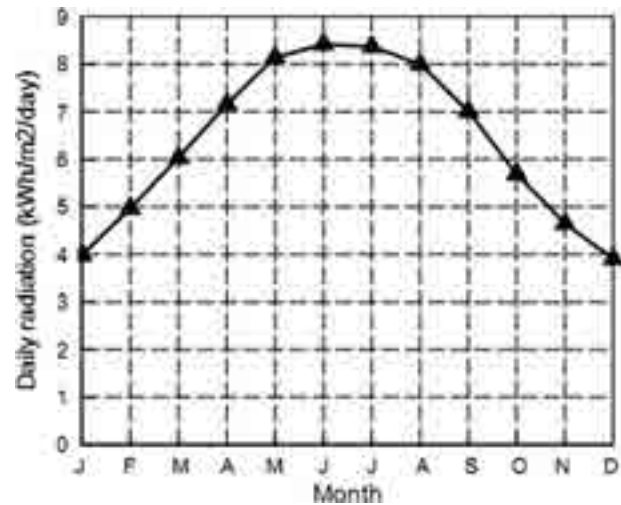


Fig. 2 Monthly average daily radiation

- -10%: Bought electricity power is 90% of sold electricity power.
- -20%: Bought electricity power is 80% of sold electricity power.

This study explains the effect of electricity power rate on these situations economically and ecologically.

3 Components of the Hybrid System

3.1 Photovoltaic Panels. The solar energy calculations are made by using the hourly solar radiation data. The electricity generated by the PV systems is directly related to the solar energy received by the PV panels, while the PV panels can be placed at different tilt angles and orientations. Most local solar observatories only provide global solar irradiation data on a horizontal plane (radiation in Kerman for different months of a year has been shown in Fig. 2).

Thus, an estimate of the total solar radiation incident on any required sloping surfaces is needed. For obtaining the beam and diffuse components of global solar radiation, the correlation of Erbs et al. is used [17]

$$\frac{I_d}{I_T} = \begin{cases} 1.0 - 0.09k_T & \text{for } k_T \leq 0.22 \\ 0.9511 - 0.1604k_T + 4.388k_T^2 & \text{for } 0.22 < k_T \leq 0.22 \\ -16.638k_T^3 + 12.336k_T^4 & \text{for } k_T > 0.8 \\ 0.165 & \end{cases} \quad (1)$$

where I_T , I_b , and I_d are global, beam, and diffuse solar radiations on a horizontal plane, respectively. k_T is hourly clearness index

$$k_T = \frac{I_T}{I_o} \quad (2)$$

where I_o is extraterrestrial radiation:

$$I_o = \frac{12 \times 3600}{\pi} G_{sc} \left(1 + 0.033 \cos \frac{360n}{365} \right) \times \left[\cos \varphi \cos \delta (\sin \omega_2 - \sin \omega_1) + \frac{\pi(\omega_2 - \omega_1)}{180} \sin \varphi \sin \delta \right] \quad (3)$$

where $G_{sc} = 1367 \text{ W/m}^2$ is solar constant, n the n th day of the year, φ the latitude, δ declination angle, and ω_1 and ω_2 are hour angles.

The beam solar radiation is the difference between global and diffuse solar radiations

$$I_b = I_T - I_d \quad (4)$$

The HDKR model (Hay–Davies–Klucher–Reindl model) is utilized to estimate the total solar radiation on the tilted surface

$$I_T = (I_b + I_d A_i) R_b + I_d (1 - A_i) \left(\frac{1 + \cos \beta}{2} \right) \left[1 + f \sin^3 \left(\frac{\beta}{2} \right) \right] + (I_b + I_d) \rho_g \left(\frac{1 - \cos \beta}{2} \right) \quad (5)$$

where A_i is the anisotropy index, and R_b is the geometric factor, which are defined as below:

$$A_i = \frac{I_b}{I_o} \quad (6)$$

$$R_b = \frac{\cos \theta}{\cos \theta_z} \quad (7)$$

In the above relations, θ and θ_z are incidence and zenith angles, respectively; f is the cloudiness factor and is given by the following equation:

$$f = \sqrt{\frac{I_b}{I_b + I_d}} \quad (8)$$

In Eq. (1), β is the slope of PV panels and ρ_g , the ground reflectance (also called Albedo), is the fraction of solar radiation incident on the ground that is reflected. A typical value of ground reflectance for grass-covered areas is 20%, snow-covered area is 70%, grass-plot area is 30%, and desert dry lands are 45%. In this article, the ground reflectance value is considered to be 45% cent according to the Kerman climate (dry/desert-covered area).

Hourly power output from PV system is given by

$$P_{PV} = I_T \eta_m \eta_{pc} P_f A_{PV} \quad (9)$$

where A_{PV} is the total area of the PV modules in m^2 , η_m is the module reference efficiency (0.11), P_f is the packing factor (0.91), and η_{pc} is the power conversion efficiency (0.83). The module

reference efficiency η_m can be estimated from the current and voltage of the PV module at maximum power point

$$\eta_m = \text{Cu}_{mp} V_{mp} / G A_{cs} \quad (10)$$

where Cu_{mp} is the current at maximum power point (A), V_{mp} is the voltage at maximum power point (V), and A_{cs} is the area of a single PV module (m^2). The solar radiation at reference condition G in Eq. (10) is 1000 W/m^2 .

3.2 Auxiliary Power Systems. In this study, diesel generator, gas generator, solid oxide fuel cell, and microgas turbine are considered as auxiliary power systems.

3.2.1 Diesel Generator. A diesel generator is the combination of a diesel engine with an electrical generator (often called an alternator) to generate electrical energy. Diesel generating sets are used in places without connection to the power grid as emergency power supply if the grid fails, as well as for more complex applications such as peak-opping, grid support, and export to the power grid. In this study, diesel generator is used as an auxiliary system for solar panels. The plan brings generator sets online and takes them off-line depending on the demands of the system at a given time.

3.2.2 Gas Generator. Natural gas generator usage should generally increase as it is the cleanest burning fossil fuel. Compared with oil and coal, natural gas generators produce lower emissions of nitrogen, sulfur, and greenhouse gasses such as carbon dioxide. Natural gas generators also do not produce a pungent odor as a gasoline or diesel-fueled one would. For people with houses powered by some natural gas, the comparison of the gas bill and the electricity bill will definitely show how much cheaper gas is. Therefore, natural gas generators are cleaner and cheaper, but they are not as efficient as diesel generators. For residential electrical power generation using natural gas, the fuel supply is already supplied, and there is no need to purchase and store extra fuel. Gas lines are already in place, delivering natural gas that can be used by power generators. The future of natural gas generators looks promising as more and more people are trying to help the environment as much as possible. Although natural gas does emit pollutants, it is much cleaner than other fuel sources. Even though natural gas is not the perfect fuel replacement, it is an appropriately cheap and clean alternative that should rise significantly in generator usage.

3.2.3 Microgas Turbine. Gas turbines use the chemical energy from fossil fuels to increase the internal energy of the working fluid in a combustor. Microturbines are touted to become widespread in distributed power and combined heat and power applications. They are one of the most promising technologies for powering hybrid electric vehicles. They range from handheld units producing less than a kilowatt, to commercial-sized systems that produce tens or hundreds of kilowatts. Basic principles of microturbine are based on microcombustion. Microturbine systems have many claimed advantages over reciprocating engine generators, such as higher power-to-weight ratio, low emissions, and few, or just one, moving part. Nevertheless, reciprocating engines overall are still cheaper when all factors are considered. Microturbines also have an additional advantage of having the majority of the waste heat contained in the relatively high temperature exhaust, making it simpler to capture, whereas the waste heat of the reciprocating engines is split between its exhaust and cooling system. However, reciprocating engine generators are quicker to respond to changes in output power requirement and are usually slightly more efficient, although the efficiency of microturbines is increasing. Microturbines also lose more efficiency at low power levels than reciprocating engines. Typical microturbine efficiency is 25% to 35%. When in a combined heat

and power cogeneration system, an efficiency rate 80% or more is commonly achieved.

3.2.4 Solid Oxide Fuel Cell. A solid oxide fuel cell is an electrochemical conversion device that produces electricity directly from oxidizing a fuel. Fuel cells are characterized by their electrolyte material; the SOFC has a solid oxide or ceramic electrolyte. Advantages of this class of fuel cells include high efficiency, long-term stability, fuel flexibility, low emissions, and relatively low cost. The largest disadvantage is the high operating temperature, which results in longer start-up times and mechanical and chemical compatibility issues. Solid oxide fuel cells are a class of fuel cells characterized by the use of a solid oxide material as the electrolyte. SOFCs use a solid oxide electrolyte to conduct negative oxygen ions from the cathode to the anode. The electrochemical oxidation of the oxygen ions with hydrogen or carbon monoxide thus occurs on the anode side. They operate at very high temperatures, typically between 500 and 1000 °C. At these temperatures, SOFCs do not require expensive platinum catalyst material, as is currently necessary for lower temperature fuel cells such as PEMFCs, and are not vulnerable to carbon monoxide catalyst poisoning. However, vulnerability to sulfur poisoning has been widely observed. Solid oxide fuel cells have a wide variety of applications from use as auxiliary power units in vehicles to stationary power generation with outputs from 100 W to 2 MW. Fuel cells were invented over a century ago and have been used in practically every NASA mission since 1960s, but until now, they have not gained widespread adoption because of their inherently high costs. Legacy fuel cell technologies such as PEMs, phosphoric acid fuel cells (PAFCs), and molten carbonate fuel cells (MCFCs) have all required expensive precious metals, corrosive acids, or hard to contain molten materials. Combined with performance that has been only marginally better than alternatives, they have not been able to deliver a strong enough economical value proposition to overcome the status quo. Some makers of legacy fuel cell technologies have tried to overcome these limitations by offering combined heat and power (CHP) schemes to take advantage of their wasted heat. While CHP does improve the economical value proposition, the cost, complexity, and customization of CHP tends to outweigh the benefits.

3.3 Inverter. A power inverter, or inverter, is an electrical device that changes direct current (DC) to alternating current (AC); the converted AC can be at any required voltage and frequency with the use of appropriate transformers, switching, and control circuits. The produced power by photovoltaic panel and solid oxide fuel cell is DC power. The stack of solid oxide fuel cell contains inverter to supply AC power. Therefore, in this study, the maximum power that must convert from DC to AC is the maximum needed load that supply by photovoltaic panels. This power is about 98 kW, and so ten 10-kW inverter with 92% efficiency have been used. If the needed load changes, number of inverters will change. Therefore, it was assumed that inverters work only with maximum efficiency.

4 Objective Functions

The objective functions are as follows:

- The annualized cost: ANC (\$/yr).
- The emissions: (kg/yr).

4.1 Annualized Cost. In finance, the annualized cost is the cost per year of owning and operating an asset over its entire lifespan. ANC is often used as a decision making tool when comparing investment projects of unequal lifespans. In the present study, to compare different configurations of economical aspects, annualized cost is used. In order to calculate ANC, annualized initial capital cost, annualized replacement cost, and annualized operating and maintenance cost will be added. Also, in this study, replacement costs are considered as 90% of initial cost.

$$\text{Annualized initial capital cost: } C_{\text{acap}} = C_{\text{cap}} \text{CRF}(i, R_{\text{proj}}) \quad (11)$$

C_{acap} , C_{cap} , CRF , i , and R_{proj} are annualized initial capital cost, initial capital cost, capital recovery factor, real interest rate, and system lifespan, respectively. System lifespan is the maximum lifespan of the hybrid system components, which, in this study, is the lifespan of PV panels (25 yr)

$$\text{Real interest rate: } i = \frac{f - i'}{f + 1} \quad (12)$$

i' and f are nominal interest rate and inflation, respectively. Real interest rate is considered equal to 6.08% for international price category [17]. Nominal interest rate and inflation for Iran price category are 18% and 24%, respectively.

$$\text{Capital recovery factor: } \text{CFR}(i, R_{\text{proj}}) = \frac{i(1+i)^{R_{\text{proj}}}}{(1+i)^{R_{\text{proj}}}-1} \quad (13)$$

Annualized replacement cost:

$$C_{\text{arep}} = C_{\text{rep}} f_{\text{rep}} \text{SFF}(i, R_{\text{comp}}) - S \cdot \text{SFF}(i, R_{\text{proj}}) \quad (14)$$

C_{arep} , C_{rep} , f_{rep} , SFF , R_{comp} , and S are annualized replacement cost, replacement cost, ratio of capital recovery factor, sinking fund factor, and lifespan of component and salvage value, respectively.

$$\text{Sinking fund factor: } \text{SFF}(i, N) = \frac{i}{(1+i)^N - 1}, \quad N = R_{\text{comp}}, R_{\text{proj}} \quad (15)$$

$$\begin{aligned} \text{Salvage value: } S &= C_{\text{rep}} \times \frac{R_{\text{rem}}}{R_{\text{comp}}}, \\ R_{\text{rem}} &= R_{\text{comp}} - (R_{\text{proj}} - R_{\text{rep}}), \\ R_{\text{rep}} &= R_{\text{comp}} \times \text{INT} \left(\frac{R_{\text{proj}}}{R_{\text{comp}}} \right) \end{aligned} \quad (16)$$

Ratio of capital recovery factor:

$$f_{\text{rep}} = \begin{cases} \text{CRF}(i, R_{\text{proj}}) / \text{CRF}(i, R_{\text{rep}}) & \text{if } R_{\text{rep}} > 0 \\ 0 & \text{if } R_{\text{rep}} = 0 \end{cases} \quad (17)$$

Operating and maintenance costs are usually annualized.

$$\text{Annualized cost: } \text{ANC} = C_{\text{acap}} + C_{\text{arep}} + C_{\text{a O M}} \quad (18)$$

Fuel prices in Iran and other places are different. In the present study, comparison is done based on two fuel prices:

- (1) Iran fuel price;
- (2) International fuel price.

Table 1 shows the price of fuel. In Iran, fuel price is multirate; so, the mean fuel prices were used. The bought electricity power rate in Iran depends on consumption (Table 2) and sold electricity power rate is about 0.023 \$/kWh. In this study, the bought and sold electricity power rate for international category are considered 0.15 \$/kWh. Table 3 shows the initial, replacement, operation, and maintenance cost of different components. This table also shows lifespan and power of the components.

Table 1 Fuel prices

	Diesel (\$/liter)	Natural gas (\$/m ³)
International	1.054	0.167
Iran	0.143	0.086

Table 2 Grid electricity power rate in Iran

Electricity power consumption (kWh)	Electricity power rate (\$/kWh)
0–100	0.0122
100–200	0.0142
200–300	0.0306
300–400	0.0551
400–500	0.0632
500–600	0.0795
>600	0.0877

4.2 Emissions. The specific fuel consumption is defined as the fuel consumption required to produce 1 kWh of energy, and it is equal to the hourly fuel consumption for supplying a given load during 1 h. According to Skarstein and Uhlen [18], the hourly fuel consumption can be approximated as follows:

$$FC = A \times P(t) + B \times P_n \quad (19)$$

where A and B are constants, $P(t)$ is the power generated at t moment, and P_n is the rated/nominal power.

Table 4 shows CO₂ and NO_x emission of different auxiliary systems for unit fuel consumption. The hours of auxiliary systems operation and, therefore, fuel consumptions are specified; so, emission of different auxiliary systems will be determined.

5 Multi-Objective Optimization Evolutionary Algorithm

In this section, the multi-objective design problem is mathematically formulated, and the basic concepts used by the MOEAs are defined. Finally, the applied MOEA (PESA) is also described, which searches the best combination of components minimizing ANC and pollutant emissions.

5.1 The Concept of a Multi-Objective Optimization. A multi-objective optimization problem can be defined as follows:

- Minimize or maximize the objective functions included in the vector:

$$F(x) = \{f_1(x), f_2(x), \dots, f_k(x)\}$$

- Satisfy the m restrictions of inequality and the p restrictions of equality:

$$g_i(x) \geq 0, \quad i = 1, 2, \dots, m$$

$$h_i(x) = 0, \quad i = 1, 2, \dots, p$$

where x is a vector whose elements are the decisive variables of the problem.

Concepts related to Pareto optimality are regularly used in most MOEAs. Because of this, the concepts of Pareto

Table 4 CO₂ and NO_x emission per unit fuel consumption for different auxiliary systems

	CO ₂ emission [26]	NO _x emission [27]
Diesel generator	2.487 (kg/liter diesel)	0.0388 (kg/liter diesel)
Solid oxide fuel cell	1.931 (kg/m ³ NG)	0.00003838 (kg/m ³ NG)
Gas generator	1.931 (kg/m ³ NG)	0.00215 (kg/m ³ NG)
Microgas turbine	1.931 (kg/m ³ NG)	0.00095 (kg/m ³ NG)

dominance, Pareto optimality, Pareto optimal set, and Pareto front are defined:

- Pareto dominance: a vector $u = (u_1, u_2, \dots, u_k)$ is said to dominate $v = (v_1, v_2, \dots, v_k)$ (denoted by $u \preceq v$) if and only if u is partially less than v , i.e., $\forall i \in \{1, 2, \dots, k\}: u_i \preceq v_i \wedge \exists i \in \{1, 2, \dots, k\}: u_i < v_i$
- Pareto optimality: a solution $x \in \Omega$ is said to be Pareto optimal with respect to Ω if and only if there is no $x' \in \Omega$ for which $v = F(x') = (f_1(x'), f_2(x'), \dots, f_k(x'))$ dominates $u = F(x) = (f_1(x), f_2(x), \dots, f_k(x))$
- Pareto optimal set: for a given multi-objective optimization problem (MOP) $F(x)$, the Pareto optimal set (P^*) is defined as follows:

$$P^* = \{x \in \Omega | \exists x' \in \Omega : F(x') \preceq F(x)\}$$

- Pareto front: for a given MOP $F(x)$ and Pareto optimal set P^* , the Pareto front (PF*) is defined as follows: PF* = $\{u = F(x) = (f_1(x), f_2(x), \dots, f_k(x)) | x \in P^*\}$

5.2 The Implemented MOEA. The implemented multi-objective algorithm is based on PESA [19] because it has relatively fast convergence, probably due to its higher elitism intensity, and it also has good accuracy. This algorithm is in charge of finding the designs that manage to, simultaneously, minimize the ANC of the system and the pollutant emissions. It has been developed using the MATLAB programming language. The algorithm (MOEA) can search for the configuration of PV panels, the auxiliary system, and the inverter, which minimizes the two objectives mentioned.

In the general, the codification of the variables used by the algorithm is done through a vector made up of two integers: i, j , where i is the number of PV panels; j is the power of auxiliary system.

In this algorithm, first, the situation for connection between the power generation system and the grid utility is elected. Then, among the configurations that follow this situation, the optimum configurations are selected by the following steps.

5.3 Steps of the Algorithm. PESA has two parameters concerning population size, i.e., PI (the size of the internal population (IP)) and PE (the maximum size of the archive or external population (EP)). It has one parameter concerning the hypergrid crowding strategy. The main steps in this algorithm are (i) generate and evaluate each of an initial IP of PI chromosomes and initialize the EP to the empty set; (ii) incorporate the nondominated members

Table 3 Specifications of different components

	Initial capital cost (\$/kW)	Replacement cost (\$/kW)	O&M cost per year (\$/kW) [20]	Lifespan (yr)
PV panel	1000–3000 [21]	0	0.0025	25
Inverter	200–400 [21]	360–450	0.0015	15
DG	150–400 [22]	135–360	0.01	20
SOFC	700–1500 [23]	2700	0.0086	15
GG	200–400 [24]	180–360	0.01	20
MGT	700–900 [25]	630–810	0.015	10

of IP into EP; (iii) if a termination criterion has reached, then stop, returning the set of chromosomes in EP as the result. Otherwise, delete the current contents of IP and repeat the following until PI new candidate solutions have been generated. With probability P_c , select two parameters from EP. Produce a single child via uniform crossover and mutate the child via bit-flip mutation. With probability $(1-P_c)$, select one parent and mutate it to produce a child; and (iv) repetition of the same process:

1. Generate and evaluate each of an initial IP of PI chromosomes.
2. Initialize the EP as empty set.
3. For $t = 1$ to number of generations
 - 3.1 Incorporate the nondominated members of IP into EP.
 - 3.2 Delete the current content of IP.
 - 3.3 Until obtaining new solution of PI.
 - 3.3.1 Select two parents from EP with probability P_c .
 - 3.3.2 Recombine this two parents for obtaining one offspring
 - 3.3.3 Mutate the offspring
 - 3.3.4 Select one parent from IP with probability $(1-P_c)$
 - 3.3.5 Mutate the parent to produce one offspring
 - 3.3.6 Add the two obtained offspring into IP
4. Return to 3

In Fig. 3, the algorithm of the computer program used for this purpose is presented.

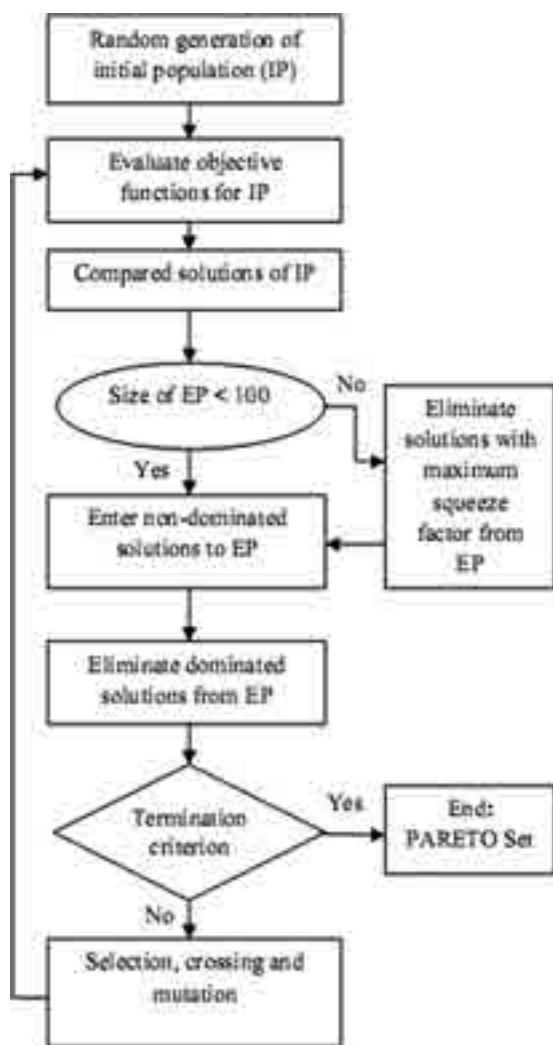


Fig. 3 PESA algorithm flowchart

6 Results

The effect of PV panel price change on using the auxiliary power system in the hybrid system in grid-connected situation has been discussed economically and ecologically in this work. In addition, different auxiliary systems are compared to select the best auxiliary power system in combination with PV panels. An evolutionary algorithm (PESA) is used for this selection purpose. Annualized cost and CO_2 emission are used as two objective functions. SOFC, DG, GG, and MGT have been used as auxiliary systems in the hybrid system. If the panel angle changes, the PV panel productivity increases and the required auxiliary power decreases; so, the annualized cost and emission are reduced. In this study, the effect of monthly and seasonal changes of the panel angle is considered. In addition, different situations for connection between power generation system and grid utility are compared. Except for the results of Sec. 6.6, the 0% situation is considered for obtaining the results. Because fuel prices in Iran vary from other areas, this comparison is made based on two fuel and electricity power rate prices: Iran's price category and the international price category.

6.1 The Hybrid System Strategy. The load demand is determined for each hour. If the generated power from PV panels is greater than the load demand, the excess power is sold to the grid utility. If the generated power from PV panels is lower than the load demand, the remaining power is generated by the auxiliary system. Finally, if the remaining power is greater than the auxiliary system power, the difference between the remaining power and the auxiliary power is bought from the grid utility. The SOFC and PV panel generated power is DC current, which is converted into the AC current by inverters.

6.2 Algorithm Parameters. The number of generations is $N_{\text{gen}} = 50$. Population is $N_m = 100$. Maximum size of the Pareto front is $N_{\text{max}} = 100$. The uniform crossover with rate = 0.7 and the bit-flip mutation set with rate = 0.003 are used. The number of panels can change from 1 to 3000. Power of the auxiliary system can be the multiples of 5 between 0 to 200 kW. Therefore, the number of possible combinations of components is $3000 \times 41 = 123,000$. Just a number of these possible combinations follow the situation for connection between the power generation system and the grid utility, and the PESA algorithm must select the optimum combinations among these specific combinations.

6.3 Effect of PV Panel Capital Cost. Figure 4 shows the effect of panel capital cost on the use of APS in the power generation system. The results of this figure are for international price category. There are three curves in this figure, each of which is related to an auxiliary power system. The PV panel capital cost is shown in horizontal axis, and the auxiliary power system capital cost is shown in vertical axis. Using the auxiliary power system is justified only in the area under the curves. For example, if the SOFC is considered as the auxiliary system and PV panels are supplied with 2000 \$/kW, using the APS decreases the ANC in case the APS capital cost is lower than 1650 \$/kW. However, if the APS capital cost is higher than that, using the auxiliary power system causes the ANC of power generation system to increase. Since APSs produce emission, using the APSs is not justified if their use increases ANC. When the PV panels are supplied with 1000 \$/kW, using the APS with even zero capital cost cannot decrease the ANC. As a result, using the APS is not justified for PV panels with capital cost lower than 1000 \$/kW. The reason for this is that the fuel consumption cost of the auxiliary power system. When the PV panel capital cost is more than 2500 \$/kW, using the APS is economic even if the APS capital cost is higher than the PV panel capital cost. Because of the discontinuous nature of solar radiation, the PV-only power generation system has to choose a more nominal power than does the PV-auxiliary

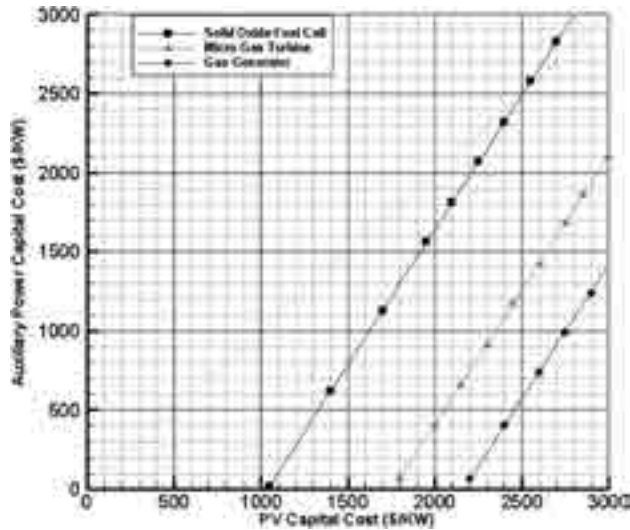


Fig. 4 Different curves that using the APS in the hybrid system is justified for points under them, international prices

system for a constant load. Furthermore, APS fuel consumption cost is low, compared to annualized capital cost; therefore, in high capital cost, the APS capital cost can be more than that of the PV panel capital cost in economic condition. The current capital cost of microgas turbine is about 800 \$/kW. Now, if the PV panels are supplied with a capital cost of more than 2250 \$/kW, using the MGT in the hybrid system is justified. If PV capital cost is lower than 1800 \$/kW, even if the MGT capital cost is zero, using the APS is not justified. The current capital cost of gas generator is about 300 \$/kW. This means that, if the PV panels are supplied with a capital cost of more than 2350 \$/kW, using the GG is economic. However, with a PV panel capital cost lower than 2200 \$/kW, using the GG in the hybrid system at any capital cost is not justified. There is not any curve for diesel generator in Fig. 4 because using the DG in hybrid system for grid-connected condition is not justified, even if the PV panels are supplied with the highest current capital cost (3000 \$/kW).

Figure 5 shows the results for Iran's price category. It is obvious that there is a curve for DG in this figure. Because of low diesel fuel price in Iran, using the DG in the hybrid system in

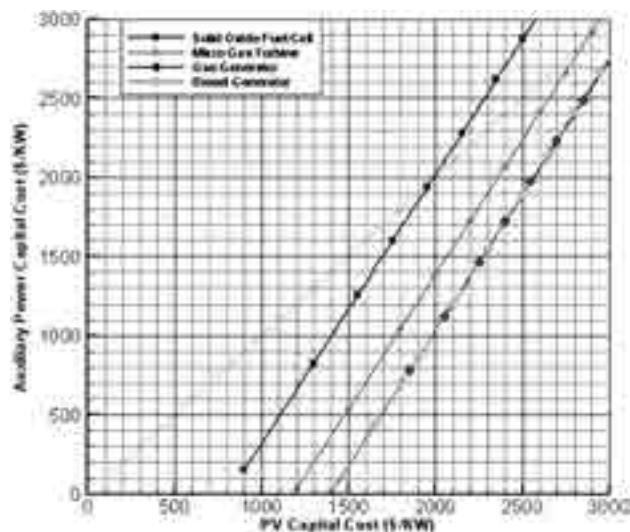


Fig. 5 Different curves that using the APS in the hybrid system is justified for points under them, Iran prices

grid-connected condition can be economic. The DG curve is, to some extent, in accordance with the GG curve. If the PV capital cost is lower than 1400 \$/kW, even if DG and GG capital cost is zero, using the APS is not justified. Using the MGT in combination with PV panels in Iran's price category is justified for current capital cost when the PV panel capital cost is more than 1650 \$/kW. The difference between various APS curves is due to the difference between the efficiency of different APSs and, therefore, the difference between their fuel consumption. The current capital cost of SOFC is between 700 and 1500 \$/kW. If the SOFC capital cost is considered about 1100 \$/kW, using the SOFC in the hybrid system is justified when the PV panel capital cost is more than 1450 \$/kW. If the fuel price decreases, using APS in the hybrid system in grid-connected condition can be economic for lower PV panel capital cost. However, due to diminishing fossil fuel resources, it is unlikely that fuel prices decrease. The effect of the fuel price increase can be determined with the comparison between the results of the international price category and Iran's price category. The fuel price in international category is higher than the fuel price in Iran category. It is obvious that using the APS in the hybrid system is justified for higher PV panel capital costs when fuel prices increase.

6.4 Selecting the Best Auxiliary System. According to the current PV panel capital cost (1000–3000 \$/kW), if PV panels are supplied with 1000 \$/kW, using the APS in the power generation system in grid-connected condition is not justified for either Iran or international price categories. To compare the different APSs in combination with PV panels in order to supply the needed load, in international price category, PV panel capital cost is considered 3000 \$/kW, and in Iran price category, PV panel capital cost is considered 2000 \$/kW.

Figure 6 shows the Pareto frontiers for the hybrid system when different power systems are used as the auxiliary power system. The PV panel capital cost is considered 3000 \$/kW, and international price category is assumed. It is obvious that the SOFC causes the least ANC in a constant CO₂ emission and the least CO₂ emission in a constant ANC. MGT provides better results than GG. Since, in international price category, using the DG in the hybrid system is not justified with 3000 \$/kW capital cost, there is not any curve for DG–PV hybrid system in this figure. Although the CO₂ production of the SOFC, MGT, and GG per unit fuel consumption is the same, the SOFC produces the least CO₂ emission because of its high efficiency. The efficiency of

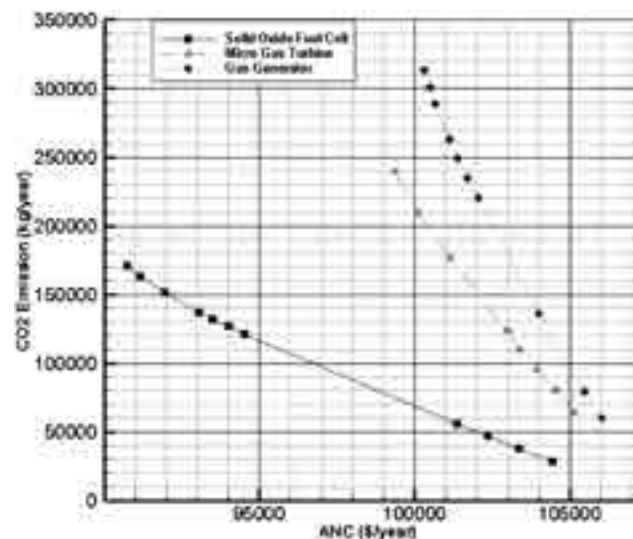


Fig. 6 Pareto frontiers of the hybrid system with different APS in CO₂-ANC coordinates for international prices

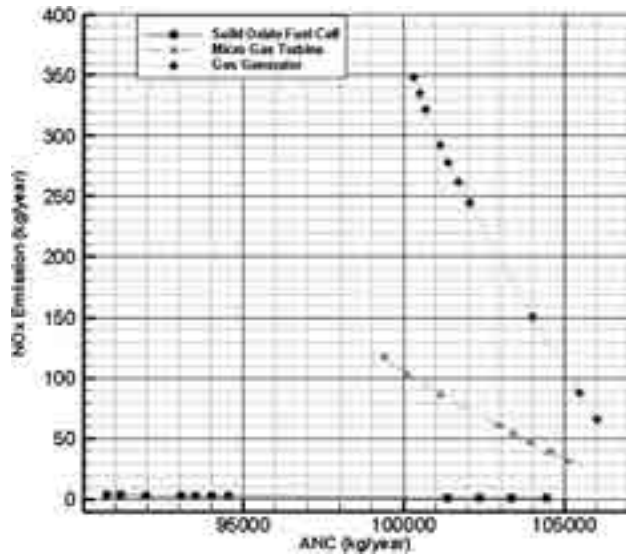


Fig. 7 Pareto frontiers of the hybrid system with different APS in NO_x-ANC coordinates for international prices

MGT is more than GG; therefore, MGT has lower CO₂ emission than GG.

Figure 7 shows the Pareto frontier in NO_x-ANC coordinates. The conditions of the hybrid systems are the same as those in Fig. 6. The SOFC-PV system causes the best result. In general, the SOFC produces the least NO_x per unit fuel consumption among these power systems. Table 5 shows two results of each Pareto frontier for comparison.

The results for Iran's price category are shown in Figs. 8 and 9. The PV capital cost is considered 2000 \$/kW in this category. Figure 8 shows the Pareto frontiers in CO₂-ANC coordinates for different hybrid systems. The SOFC-PV system is again the best hybrid system economically and ecologically. The DG causes better results than MGT and GG because it has better efficiency and, therefore, less fuel consumption. Although the SOFC has the most capital cost, it has the highest efficiency. Therefore, the SOFC uses less fuel for a constant power than others. It is obvious that MGT causes less acceptable results than GG in these conditions. Since Iran's natural gas price is less than international NG price, the influence of fuel consumption in the ANC is low in Iran's price category. Therefore, because the capital cost of MGT is higher than GG, the ANC of MGT-PV system is approximately higher than GG-PV system.

Figure 9 shows the Pareto frontiers in NO_x-ANC coordinates. The DG-PV system causes the least favorable results. The reason could be the type of fuel and the operating temperature. The fuels with large carbon chain and high operating temperature make good conditions for nitrogen oxides production. Some of the multi-objective optimization algorithm results are shown in Table 6 for comparison.

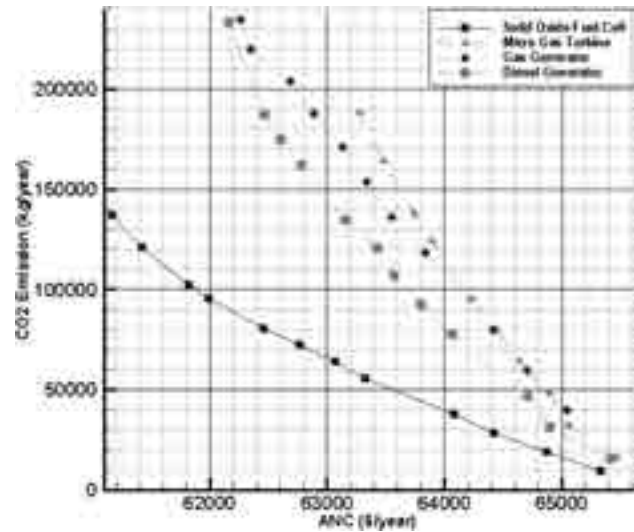


Fig. 8 Pareto frontiers of the hybrid system with different APS in CO₂-ANC coordinates for Iran prices

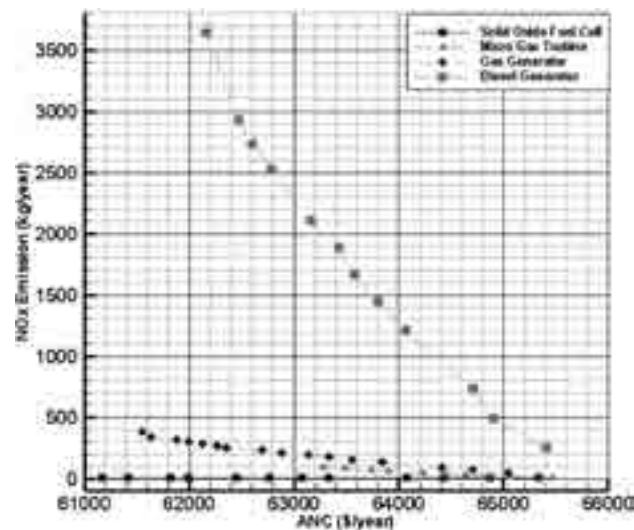


Fig. 9 Pareto frontiers of the hybrid system with different APS in NO_x-ANC coordinates for Iran prices

6.5 Effect of Panel Angle Change. If the received solar radiation on the PV panel increases, the generating PV panel power increases. If the panel angle changes and tracks the sun, PV panel productivity increases and the number of panels decreases; so, the annualized cost and emission are reduced. In this study, the effect of seasonal and monthly panel angle changes is considered. The best panel angle in Kerman (30°15'N, 56°58'E), Iran, for the most productivity in different months and seasons are brought in

Table 5 Some of the optimum results for international price category

	ANC (\$/yr)	Fuel consumption (m ³ /yr)	CO ₂ emission (kg/yr)	NO _x emission (kg/yr)	No. panel	Power of APS (kW)
SOFC-PV hybrid system	103,380.2	19,538.11	37,728.09	0.749873	2293	20
	93,076.12	70,961.06	137,025.8	2.723485	1659	90
MGT-PV hybrid system	105,130.4	33,406.48	64,507.91	31.73615	2293	20
	99,399.56	124,073.6	239,586.2	117.87	1659	90
GG-PV hybrid system	105,486.6	41,187.15	79,532.4	88.55238	2293	20
	100,503.6	155,950.5	301,140.5	335.2936	1658	90

Table 6 Some of the optimum results for Iran price category

	ANC (\$/yr)	Fuel consumption	CO ₂ emission (kg/yr)	NO _x emission (kg/yr)	No. panel	Power of APS (kW)
SOFC–PV hybrid system	64,871.96	9,796.576 (m ³ /yr)	18,917.19	0.375993	2398	10
	61,995.75	49,366.56 (m ³ /yr)	95,326.84	1.894689	1924	55
MGT–PV hybrid system	65,064.22	16,741.76 (m ³ /yr)	32,328.35	15.90468	2391	10
	63,485.67	85,107.31 (m ³ /yr)	164,342.2	80.85195	1923	55
GG–PV hybrid system	65,046.03	20,629.7 (m ³ /yr)	39,835.95	44.35386	2398	10
	62,690.4	105,679.5 (m ³ /yr)	204,067.2	227.211	1925	55
DG–PV hybrid system	64,901.93	12,495 (liter/yr)	31,074.1	485.275	2390	10
	62,788.11	64,999.46 (liter/yr)	161,648.6	2524.418	1925	55

Table 7 Best tilt angle for different months of a year

Month	1	2	3	4	5	6	7	8	9	10	11	12
Panel tilt angle	55	50	35	20	10	10	10	15	30	45	55	60

Table 8 Best tilt angle for different seasons of a year

Season	Winter	Spring	Summer	Autumn
Panel tilt angle	45	10	15	55

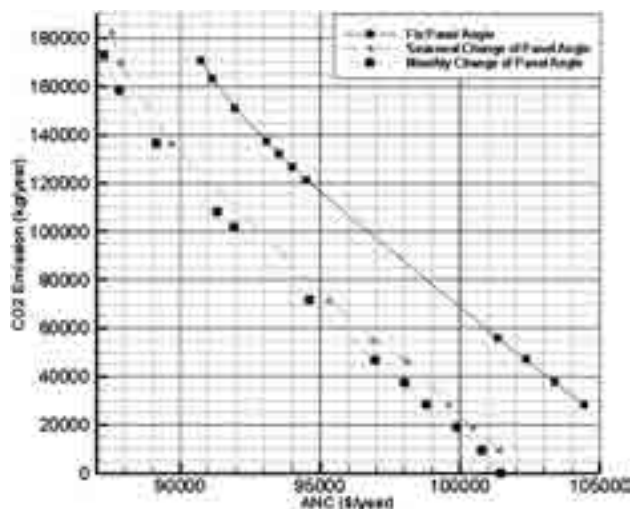


Fig. 10 Pareto frontiers of the SOFC–PV hybrid system for fix panel angle, seasonal panel angle change, and monthly panel angle change: international prices

Tables 7 and 8. The optimum panel angle in Kerman for fixed panel angle situation is 30 deg.

Figure 10 shows the effect of panel angle change for PV–SOFC hybrid system in international price category. It is obvious that monthly panel angle change gives better results than others, but the difference between the monthly change results and the seasonal change results is little. Figure 11 shows the Pareto frontiers for PV–SOFC system in Iran’s price category. The result is the same as the previous situation.

6.6 Effect of Different Situation for Connection Between Hybrid System and Grid Utility. Different situations for connection between power generation system and grid utility are compared in Fig. 12. The Pareto frontiers for different situations in international price category are plotted for SOFC–PV hybrid

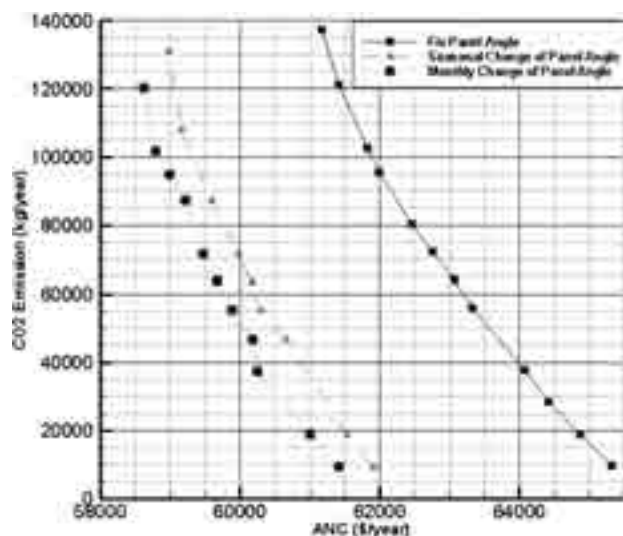


Fig. 11 Pareto frontiers of the SOFC–PV hybrid system for fix panel angle, seasonal panel angle change, and monthly panel angle change: Iran prices.

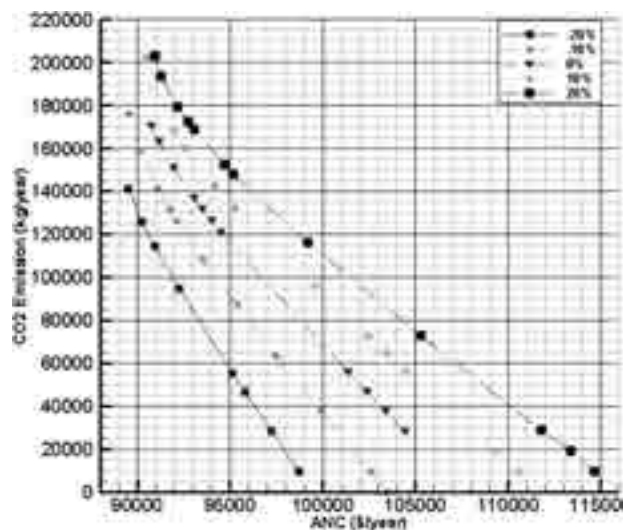


Fig. 12 Pareto frontiers of the SOFC–PV hybrid system for different situations of grid and power generation system connection: international prices

system. It is obvious that the –20% situation causes the best results. This means that, if the power generation system generates more power and the sold power is more than the bought power, the ANC of the hybrid system decreases. The reason is that the

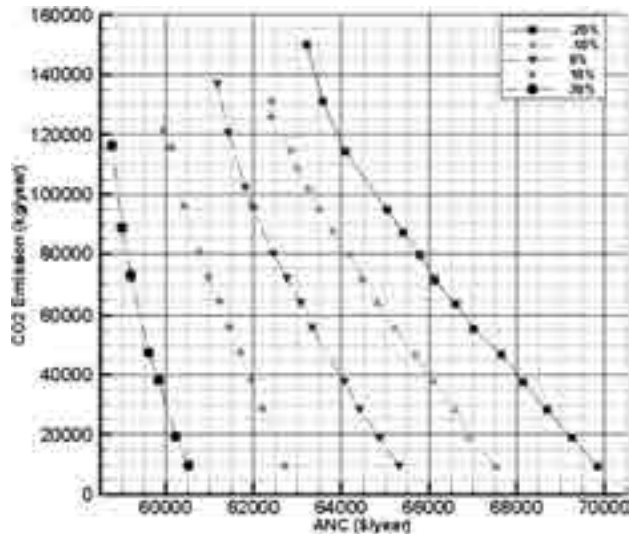


Fig. 13 Pareto frontiers of the SOFC–PV hybrid system for different situations of grid and power generation system connection: Iran prices

cost of unit power generation with the hybrid system is less than that of the unit power from the grid.

Figure 13 shows the Pareto frontiers for different situations in Iran's price category. It is obvious that 20% situation causes the least ANC in a constant CO₂ emission and the least CO₂ emission in a constant ANC. The reason is that the unit power generation cost with the hybrid system is higher than the grid unit power cost. The other hybrid systems cause result similar to these of the SOFC–PV hybrid system.

7 Conclusion

Using an auxiliary power system in combination with the PV panels to supply a sample load demand in grid-connected condition depends on fuel price, solar radiation intensity, number of solar days, PV panel capital cost, and the APS capital cost. It is probable that, because of the diminishing resources of fossil fuels, the fuel prices will not decrease. Therefore, if PV panels are supplied with a capital cost less than 1000 \$/kW, using the APS in combination with PV panels for grid-connection power generation is not justified. This result is for Kerman, which has high solar radiation intensity and large number of solar days. For places with lower solar radiation intensity or smaller number of solar days, using the APSs with PV panels for power generation can be justifiable for lower PV panel capital cost. For places with higher solar radiation intensity or larger number of solar days, the use of APSs may not be justifiable for even higher PV panels capital cost. If the capital cost of PV panels and APS are in a range in which using the APS in the hybrid system is justified, the best auxiliary power system in combination with PV panels for power generation is solid oxide fuel cell. Solid oxide fuel cell with high efficiency and low emission is the best APS economically and ecologically. Panel angle change can reduce the annualized cost of the system. According to results, the difference between the monthly panel angle change results and the seasonal panel angle change results is little. Because the number of panels is high and

changing their angle monthly is difficult, the seasonal panel angle is recommended. The best situation for connection between the grid utility and the power generation hybrid system depends on the unit electricity power price of the grid.

References

- [1] Bernal-Agust, J. L., and Dufo-Lopez, R., 2009, "Simulation and Optimization of Stand-Alone Hybrid Renewable Energy Systems," *Renewable Sustainable Energy Rev.*, **13**(8), pp. 2111–2118.
- [2] Baniasad Askari, I., and Ameri, M., 2009, "Optimal Sizing of Photovoltaic-Battery Power Systems in a Remote Region in Kerman, Iran," *Proc. Inst. Mech. Eng., Part A*, **223**, pp. 563–570.
- [3] Dufo-Lopez, R., and Bernal-Agust, J. L., 2005, "Design and Control Strategies of PV-Diesel Systems Using Genetic Algorithms," *Sol. Energy*, **79**(1), pp. 33–46.
- [4] Lau, K. Y., Yousof, M. F. M., Arshad, S. N. M., Anwar, M., and Yatim, A. H. M., 2010, "Performance Analysis of Hybrid Photovoltaic/Diesel Energy System Under Malaysian Conditions," *Energy*, **35**, pp. 3245–3255.
- [5] Baniasad Askari, I., and Ameri, M., 2011, "The Effect of Fuel Price on the Economic Analysis of Hybrid (Photovoltaic/Diesel/Battery) System in Iran," *Energy Sources, Part B*, **6**, pp. 357–377.
- [6] Tudorache, T., and Morega, A., 2008, "Optimum Design of Wind/PV/Diesel/Batteries Hybrid Systems," Second International Conference on Modern Power Systems, Romania.
- [7] Degobert, Ph., Kreuawanand, S., and Guillaud, X., 2006, "Micro-Grid Powered by Photovoltaic and Micro Turbine," International Conference on Renewable Energies, France.
- [8] Sergio, B., Silva, S. B., de Oliveira, M. A. G., and Severino, M. M., 2010, "Economic Evaluation and Optimization of a Photovoltaic–Fuel Cell–Batteries Hybrid System for Use in the Brazilian Amazon," *Energy Policy*, **38**, pp. 6713–6723.
- [9] Eroglu, M., Dursun, E., Sevencan, S., Song, J., Yazici, S., and Kilic, O., 2011, "A Mobile Renewable House Using PV/Wind/Fuel Cell Hybrid Power System," *Int. J. Hydrogen Energy*, **36**, pp. 7985–7992.
- [10] Roth-Deblon, A., 2006, "Combined DC and AC Integration of Energy Sources in Hybrid 3-Phase Off-Grid Systems," 4th World Conference on Photovoltaic Energy Conversion (IEEE, 2006), 2, pp. 2431–2433.
- [11] Kjaer, S. B., Pedersen, J. K., and Blaabjerg, F., 2005, "A Review of Single-Phase Grid-Connected Inverters for Photovoltaic Modules," *IEEE Trans. Ind. Appl.*, **41**(5), pp. 292–306.
- [12] Türkay, B. E., and Telli, A. Y., 2011, "Economic Analysis of Standalone and Grid Connected Hybrid Energy Systems," *Renewable Energy*, **36**, pp. 1931–1943.
- [13] Liu, G., Rasul, M. G., Amanullah, M. T. O., and Khan, M. M. K., 2012, "Techno-Economic Simulation and Optimization of Residential Grid-Connected PV System for the Queensland Climate," *Renewable Energy*, **45**, pp. 146–155.
- [14] Bernal-Agust, J. L., and Dufo-Lopez, R., 2009, "Multi-Objective Design and Control of Hybrid Systems Minimizing Costs and Unmet Load," *Electr. Power Syst. Res.*, **79**, pp. 170–180.
- [15] Dufo-Lopez, R., and Bernal-Agust, J. L., 2008, "Multi-Objective Design of PV–Wind–Diesel–Hydrogen–Battery Systems," *Renewable Energy*, **33**, pp. 2559–2572.
- [16] Sadeghi, S., and Ameri, M., 2012, "Multi-Objective Optimization of PV-Battery Power Systems," 20th Annual International Conference on Mechanical Engineering of Iran.
- [17] Erbs, D. G., Klein, S. A., and Duffie, J. A., 1982, "Estimation of the Diffuse Radiation Fraction for Hourly, Daily, and Monthly-Average Global Radiation," *Solar Energy*, **28**(4), pp. 293–302.
- [18] Arun, P., Banerjee, R., and Bandyopadhyay, S., 2008, "Optimum Sizing of Battery-Integrated Diesel Generator for Remote Electrification Through Design-Space Approach," *Energy*, **33**, pp. 1155–1168.
- [19] Corne, W., Knowles, D., and Oates, J., 2000, "The Pareto Envelope-Based Selection Algorithm for Multi Objective Optimization," *J. Lect. Notes Comput. Sci.*, **1917**, pp. 839–848.
- [20] Mekhilef, S., Saidurb, R., and Safari, A., 2012, "Comparative Study of Different Fuel Cell Technologies," *Renewable Sustainable Energy Rev.*, **16**, pp. 981–989.
- [21] <http://www.wholesalesolar.com/>
- [22] <http://www.hardydiezel.com/>
- [23] Seattle City Light 2010 Integrated Resource Plan/Appendix I
- [24] http://www.lowes.com/Electrical/Generators/Home-Standby-Generators/_/N-1z0x2n8/pl#!
- [25] <http://www.wbdg.org/resources/microturbines.php>
- [26] <http://www.eia.gov/tools/faqs/faq.cfm?id=73&t=11>
- [27] Wu, D., W., and Wang, R., Z., 2006, "Combined Cooling, Heating and Power: A Review," *Prog. Energy Combust. Sci.*, **32**, pp. 459–495.